BIOMATERIALS

10.1126/sciadv.1600102

The transition from linear to highly branched poly(β-amino ester)s: Branching matters for gene delivery

Dezhong Zhou,[1,2]* Lara Cutlar,[2]* Yongsheng Gao,[2]* Wei Wang,[2] Jonathan O'Keeffe-Ahern,[2] Sean McMahon,[2] Blanca Duarte,[3] Fernando Larcher,[3] Brian J. Rodriguez,[4] Udo Greiser,[2] Wenxin Wang[1,2]†

Nonviral gene therapy holds great promise but has not delivered treatments for clinical application to date. Lack of safe and efficient gene delivery vectors is the major hurdle. Among nonviral gene delivery vectors, poly(β-amino ester)s are one of the most versatile candidates because of their wide monomer availability, high polymer flexibility, and superior gene transfection performance both in vitro and in vivo. However, to date, all research has been focused on vectors with a linear structure. A well-accepted view is that dendritic or branched polymers have greater potential as gene delivery vectors because of their three-dimensional structure and multiple terminal groups. Nevertheless, to date, the synthesis of dendritic or branched polymers has been proven to be a well-known challenge. We report the design and synthesis of highly branched poly(β-amino ester)s (HPAEs) via a one-pot "A2 + B3 + C2"–type Michael addition approach and evaluate their potential as gene delivery vectors. We find that the branched structure can significantly enhance the transfection efficiency of poly(β-amino ester)s: Up to an 8521-fold enhancement in transfection efficiency was observed across 12 cell types ranging from cell lines, primary cells, to stem cells, over their corresponding linear poly(β-amino ester)s (LPAEs) and the commercial transfection reagents polyethyleneimine, SuperFect, and Lipofectamine 2000. Moreover, we further demonstrate that HPAEs can correct genetic defects in vivo using a recessive dystrophic epidermolysis bullosa graft mouse model. Our findings prove that the A2 + B3 + C2 approach is highly generalizable and flexible for the design and synthesis of HPAEs, which cannot be achieved by the conventional polymerization approach; HPAEs are more efficient vectors in gene transfection than the corresponding LPAEs. This provides valuable insight into the development and applications of nonviral gene delivery and demonstrates great prospect for their translation to a clinical environment.

INTRODUCTION

Gene therapy has potential to be one of the most important fields in medicine, offering the prospect of treatment for various inherited and/or acquired diseases (*1*, *2*). Nonetheless, the translation of gene therapy treatments to clinical applications has been severely hampered because of insertional mutagenesis of virus-based systems and shortcomings in efficiency observed in non–virus-based systems (*3*, *4*), which continues to drive the development of advanced gene delivery vectors (*5*, *6*). Nonviral vectors, particularly cationic polymers, hold significant potential for translation to clinical application (*6*–*9*). The inexpensive synthesis, facile purification, and scalability of nonviral vectors coupled with demonstrated high transfection efficiency and low cytotoxicity make them highly appealing candidates for clinical applications (*10*–*12*).

Advancements in polymer chemistry have led to the design and development of various vectors with different polymeric structures (*7*, *8*). Most notable among them, linear poly(β-amino ester)s (LPAEs) have emerged as one type of the most versatile gene delivery vectors (*13*). Since they were first developed in 2000 by Lynn and Langer (*13*), more than 2500 LPAEs have been designed, synthesized, and screened by Green *et al.* (*14*), and Anderson *et al.* (*15*). Of these, the best-performing C32 series have been identified for both in vitro and in vivo gene delivery (*16*–*18*), which can even rival adenovirus on human umbilical vein endothelial cells (*18*). To date, all design, synthesis, and transfection studies with poly(β-amino ester)s have been focused on their linear structure. Although the results from LPAEs are very encouraging, the potential for synthesizing and optimizing structures with multiple functional groups is limited by the linear nature of these polymers.

Branched polymers have a three-dimensional (3D) architecture with multiple functional terminal groups, making them increasingly appealing for biomaterial applications (*4*, *19*, *20*). It is widely reported that both composition and structure can be readily manipulated to introduce a number of different functional properties (*21*–*24*). Previous investigations have demonstrated that branched structures can significantly enhance the interaction of polymers with DNA and considerably improve the formation of polymer/DNA polyplexes, protect the encapsulated DNA from degradation by endosomal enzymes, and increase the cellular uptake of polymer/DNA polyplexes, compared to linear structures (*21*, *24*–*26*). Branched polyethyleneimine (PEI) (*25*), branched poly-L-lysine (PLL) (*24*, *26*), branched poly[2-(dimethylamino)ethyl methacrylate] (PDMAEMA) (*4*), and branched glycopolymers (*19*) have all shown to perform better than their corresponding linear counterparts in transfection efficiency. Therefore, it is conceivable that highly branched poly(β-amino ester)s (HPAEs) could outperform LPAEs as nonviral gene delivery vectors, and, thus, the development of HPAEs is imperative.

Despite their obvious potential, no HPAEs were developed from the same libraries of commercially available monomers (in contrast to the more than 2500 LPAEs) because the synthesis of highly branched polymers has been a significant challenge to date (*20*, *21*). Previously, only

[1]School of Materials and Engineering, Tianjin University, Tianjin 300072, China. [2]Charles Institute of Dermatology, School of Medicine and Medical Science, University College Dublin, Dublin 4, Ireland. [3]Cutaneous Diseases Modelling Unit, Division of Biomedicine, Centro de Investigaciones Energéticas Medioambientales y Tecnológicas (CIEMAT), Madrid 28040, Spain. [4]School of Physics and Conway Institute of Biomolecular and Biomedical Research, University College Dublin, Dublin 4, Ireland.
*These authors contributed equally to this work.
†Corresponding author. Email: wenxin.wang@ucd.ie

very few HPAEs have been synthesized with the "A2 + BB′B″"–type Michael addition using very special sets of monomers or under very strict reaction conditions (in the presence of a special catalyst or under high pressure) (*20*, *27*). This severely limited the choice of branched structures, functionalities, and, ultimately, transfection capability (*28*). HPAE-containing polymers were also synthesized using low–molecular weight PEI and diacrylates (1,3-butanediol diacrylate and 1,6-hexanediol diacrylate) by Forrest *et al.* (*29*); however, the main component of these polymers was PEI instead of β-amino esters (generated via the Michael addition of amines and acrylates). Therefore, it is highly desirable to synthesize HPAEs of various compositions and structures from readily available commercial monomers using a reliable, generalizable, and flexible synthesis strategy. Here, we report the design and synthesis of HPAEs via a new one-pot "A2 + B3 + C2" Michael addition approach (Fig. 1). The HPAEs are essentially derived from the same sets of monomers as the LPAEs that have already been proven to

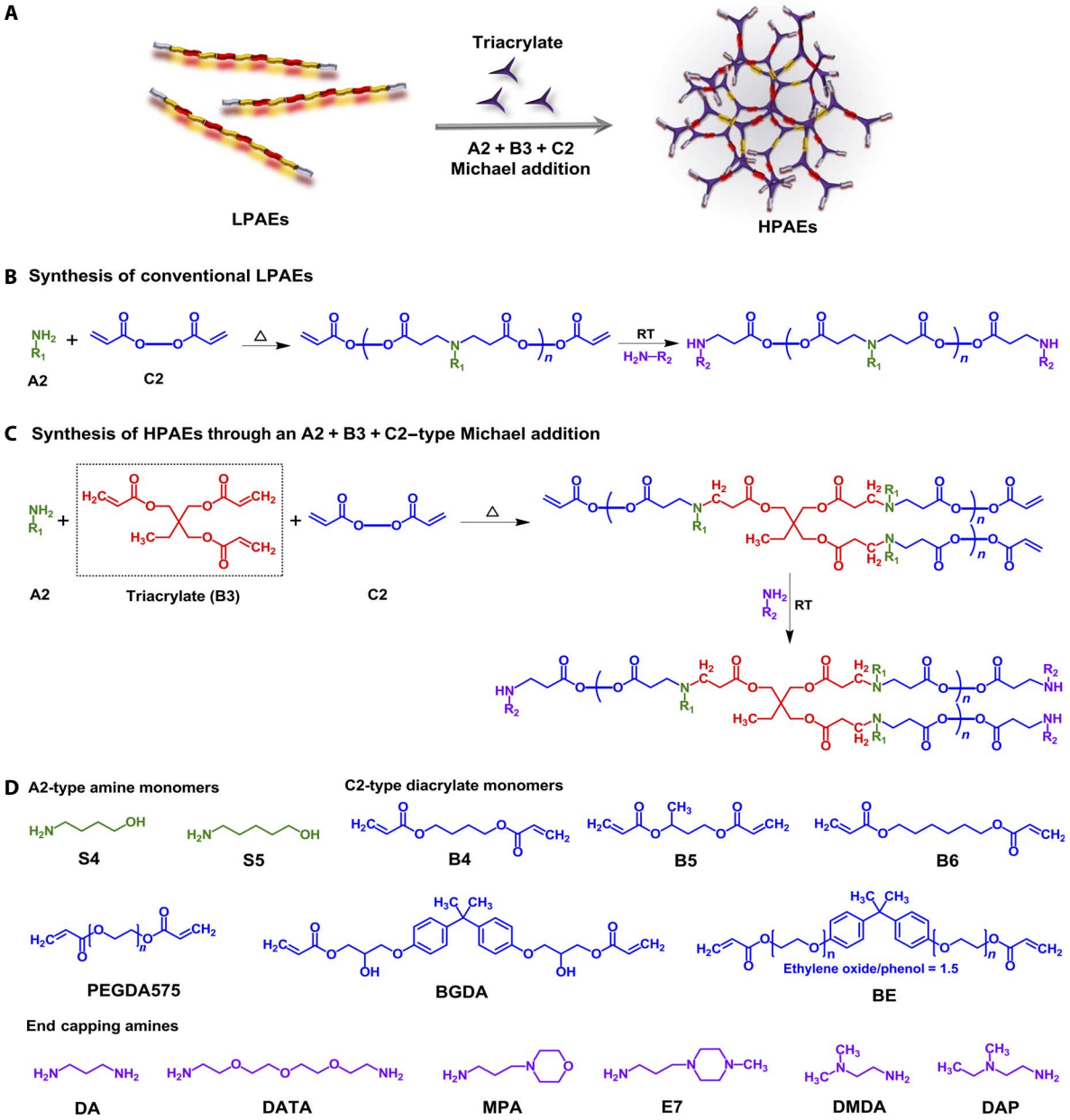

Fig. 1. Branched poly(β-amino ester)s (HPAEs) are developed via an A2 + B3 + C2 Michael addition approach from various commercially available monomers. (**A**) Scheme illustration of the development of HPAEs by branching LPAEs with triacrylate via the A2 + B3 + C2 Michael addition approach. (**B**) Scheme of the synthesis of conventional LPAEs. RT, room temperature. (**C**) Scheme of the synthesis of HPAEs. An A2-type monomer is copolymerized with a B3-type monomer and a C2-type monomer via the A2 + B3 + C2 Michael addition to first generate the acrylate-terminated base polymer and then end-capped with a second amine. (**D**) Structures of the monomers used for the synthesis of HPAEs and the corresponding LPAEs in this work. Detailed sets of monomers are listed in tables S1 and S3.

be efficient in gene delivery. Meanwhile, substantially new benefits could be obtained through the introduction of branched structures and thus give rise to much higher transfection efficiency compared to the original LPAEs, from which the HPAEs were modeled. To demonstrate the broad applicability of the A2 + B3 + C2 synthesis strategy, we first synthesized 12 HPAEs using 12 different sets of commercial monomers. Notably, six of them were previously used for the synthesis of the best-performing LPAEs-the C32 series by Akinc *et al.* (*16*), Green *et al.* (*17*), and Eltoukhy *et al.* (*18*). To validate our rationale and hypothesis and also to improve our understanding of the possible mechanisms behind the enhancement of gene transfection efficiency by the branched architecture, we further systematically tested and compared the representative HPAEs and the corresponding LPAEs regarding DNA binding, condensation, protection, buffering capacity, and cellular uptake of polyplexes, which are the major bottlenecks in gene transfection (*18*). Representative polyplex morphologies were also investigated with transmission electron microscopy (TEM) and atomic force microscopy (AFM). To investigate the effect of various branched structures on transfection efficiency, 10 HPAEs from the same sets of monomers but differing in branched structure were further synthesized. For optimal comparison and for benchmarking the high performance of poly(β-amino ester)s, the transfection efficiency of HPAEs was assessed systematically in vitro and compared to both LPAEs and the commercial transfection reagents PEI, SuperFect, and Lipofectamine 2000. *Gaussia* luciferase (Gluciferase) and green fluorescent protein (GFP) expression were used as reporters for the transfection of cells. Efficiency was assessed across 12 different cell types including epithelial cells (HKC8), fibroblasts (COS7 and 3T3), keratinocytes (NHK and RDEBK), cancer cells (HeLa and HepG2), stem cells [rat adipose-derived stem cell (rADSC) and human ADSC (hADSC)], and astrocytes (SHSY-5Y, Neu7, and primary astrocytes). Finally, the top-performing HPAE was further used to deliver the gene COL7A1 to restore the expression of the type VII collagen (C7) in a nude mouse model with human recessive dystrophic epidermolysis bullosa (RDEB) skin graft to prove the application of HPAEs as a gene delivery vector to enhance wound healing.

RESULTS

HPAE synthesized via an A2 + B3 + C2 Michael addition approach

Despite its well-established structural advantages, the synthesis of highly branched polymers remains challenging, given that uncontrolled polymerization can easily lead to gelation; in addition, the 3D structure and composition must be well tailored to maximize the functionalities and performance of the polymers (*20*). The scheme for the A2 + B3 + C2 Michael addition approach is based on the copolymerization of amine (A2) to triacrylate (B3) and diacrylate (C2) (Fig. 1). This particular chemistry allows the branching monomers (triacrylates) to combine the linear segments generated from diacrylates and amines, resulting in a branched structure. By endcapping, additional functional groups were then introduced to further enhance the property and functionalities of HPAEs as gene vectors. The A2 + B3 + C2 strategy offers multiple advantages over previously reported approaches for branched polymer synthesis: first, it uses the equal reactivity of multiple reactive groups in monomers to yield more favorable formations of highly branched polymers compared to the conventional A2 + BB′B″ and "A3 + 2BB′B" approaches (*3*, *30*–*33*); second, it decreases the risk of gelation by reducing cross-linking monomer concentration in comparison with the conventional "A2 + B3" strategy (*34*); third, it eliminates the need for special sets of monomers and thus potentiates the generation of structurally diverse branched polymers from various affordable and commercially available monomers (*30*, *35*); and, most importantly, through this approach, the structure of branched polymers can be well tailored to suit broad applications by a simple adjustment of the feed ratio of A2, B3, and C2. Using this versatile A2 + B3 + C2 branching platform, we first synthesized 12 structurally diverse HPAEs (Fig. 1D and tables S1 and S2) from the commercially available monomers that were previously proven to be effective components of LPAE vectors. For comparison, the corresponding linear counterparts (12 LPAEs) were also prepared according to previous reports (tables S3 and S4) (*17*, *18*, *36*). Monomer sets in group 2 outlined in table S3 have been repeatedly reported for the synthesis of the top-performing LPAEs—the C32 series (*18*).

Gel permeation chromatography (GPC) was used to monitor the growth of polymers during polymerization. Molecular weights [M_w (weight-average) and M_n (number-average); tables S5 and S6] of all polymers increased gradually without the occurrence of gelation (figs. S1 and S2). After endcapping, the HPAEs were highly soluble in dimethyl sulfoxide (DMSO), and their M_w ranged from 7600 to 25,000 with polydispersity index (PDI) values between 3.2 and 5.9 (tables S7 and S8 and figs. S3 and S4). The Mark-Houwink (MH) plot α values were between 0.27 and 0.47 (fig. S5), which were much lower than those of the LPAEs (between 0.5 and 0.75), demonstrating their branched structures. Nuclear magnetic resonance spectroscopy (^{1}H NMR; fig. S6) further confirmed the successful copolymerization of A2, B3, and C2 monomers. Together, these results demonstrate that the A2 + B3 + C2 Michael addition is a highly generalizable and reliable approach for controlled synthesis of HPAEs from various commercially available monomers, even at a high monomer concentration (500 mg/ml) and at a high reaction temperature (90°C).

Superiority of HPAEs in gene delivery compared with LPAEs

HeLa, rADSC, and SHSY-5Y cells were used to evaluate the gene transfection capability of the HPAEs and LPAEs. To bolster our comparison, two commercial dendritic or branched gene transfection reagents, branched PEI (M_w = 25,000) and SuperFect, along with the most widely used Lipofectamine 2000, were used as positive controls. Previous studies by Green *et al.* (*13*) and Eltoukhy *et al.* (*17*) indicated that optimal formulations for efficient gene transfection of LPAEs usually tend to have polymer/DNA weight ratios (w/w) greater than 20:1; therefore, 20:1 and 50:1 (w/w) were first used to evaluate the gene transfection efficiency of various HPAEs and LAPEs, whereas commercial gene transfection reagents were used as per optimized protocols. Gluciferase activity of cells after treatment with HPAEs and LPAEs is shown in Fig. 2 (A to C) and fig. S7. Analysis of the results revealed several trends: (i) overall, HPAEs exhibited higher transfection efficiency than the corresponding LPAEs at both w/w ratios; (ii) for HPAEs, enhancement in gene transfection efficiency at 20:1 (w/w) was stronger than that at 50:1 (w/w); (iii) highly branched S4-TMPTA-B6-MPA, S4-TMPTA-BE-MPA, and S4-TMPTA-BGDA-MPA showed the strongest enhancement in transfection efficiency among all 12 HPAEs tested. Even when compared to linear S5-B4-DA, S5-B4-DATA, and S5-B4-E7, which are the most efficient linear C32 series reported previously (*13*, *18*), the transfection efficiency of the corresponding HPAE counterparts remained higher. The 12 HPAEs developed here were derived from the same sets of monomers as the corresponding 12 LPAEs, including the linear C32 series, and

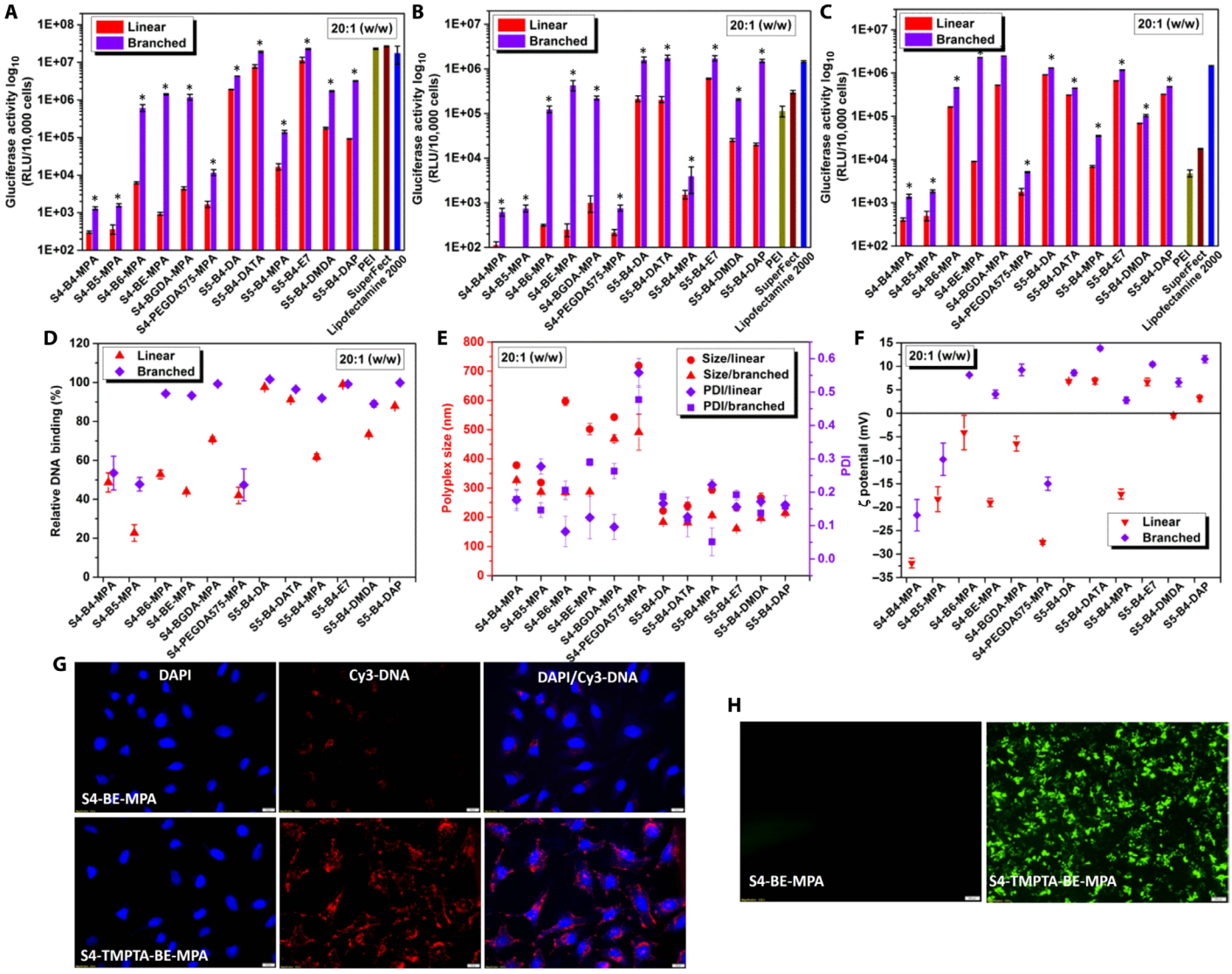

Fig. 2. HPAEs show great superiority in gene transfection compared with the corresponding LPAEs. (**A** to **C**) HeLa, rADSC, and SHSY-5Y cells show higher Gluciferase activity after treatment with HPAEs compared with the corresponding LPAEs. RLU, relative light units. (**D**) HPAEs demonstrate stronger DNA binding affinity compared with the corresponding LPAEs. (**E**) HPAEs condense DNA to allow for the formulation of smaller polyplexes with low PDI, compared to the corresponding LPAEs. (**F**) Correspondingly, HPAE/DNA polyplexes have a relatively higher ζ potential. (**G**) Fluorescence images show that the highly branched S4-TMPTA-BE-MPA mediates much higher cellular uptake of polyplexes compared with the linear counterpart S4-BE-MPA. Scale bars, 20 μm. (**H**) GFP fluorescence images show that the highly branched S4-TMPTA-BE-MPA mediates much higher gene transfection efficiency compared with the linear counterpart S4-BE-MPA. Scale bars, 200 μm. Data points marked with asterisks are statistically significant relative to the corresponding LPAEs (*$P < 0.05$; *t* test, single-tailed).

had similar molecular weights and chemical compositions; thus, the enhancement in gene transfection of HPAEs can only be attributed to the introduction of a branched structure, which demonstrates that branching can enhance gene transfection—a result that is further supported by the improvement of the gene transfection efficiency of poly(β-amino ester)s, regardless of whether they have been derived from underperforming or even from not performing linear structures. Notably, after branching, several underperforming LPAEs (for example, linear S4-B6-MPA, S4-BE-MPA, and S4-BGDA-MPA) even achieved superiority to the commercial gene transfection reagents (Fig. 2, B and C, and fig. S7), strongly emphasizing the critical role of branching in conferring poly(β-amino ester) high efficiency in gene delivery. The enhancements in gene transfection by branching were also demonstrated by the expression of GFP (Fig. 2H and fig. S8). Given that the majority of more than 2500 LPAEs were inefficient or underperforming in gene transfection (*13*), it is anticipated that, by introduction of a branched structure, a new library of much more efficient gene delivery vectors could be developed. Alamarblue assays further showed that all HPAEs can preserve high cell viability (fig. S9).

In addition to transfection efficiency, we tested possible parameter characteristics and mechanistic steps that may contribute to the

improvement of transfection efficiency obtained by branching. To this end, several analyses on polymers and polyplexes were performed. PicoGreen assays showed that, compared with LPAEs, the corresponding HPAEs were found to bind DNA with substantially higher affinity and have stronger DNA condensation ability (Fig. 2E and figs. S10A and S11A). Here, the relative DNA binding of linear S4-B6-MPA, S4-BE-MPA, and S4-BGDA-MPA was only 50, 40, and 70%, respectively, when a ratio of 20:1 (w/w) was applied. In contrast, the relative DNA binding was more than 90% in their branched counterparts, S4-TMPTA-B6-MPA, S4-TMPTA-BE-MPA, and S4-TMPTA-BGDA-MPA. Gel electrophoresis further shows that the highly branched S4-TMPTA-BE-MPA can effectively condense DNA at a ratio of 10:1 (w/w), in contrast to the ratio of greater than 30:1 for the linear S4-BE-MPA (fig. S11A). Previously, Akinc *et al.* (*16*) and Green *et al.* (*18*) have demonstrated that modification of terminal groups of LPAE (C32) from alcohol to primary amines can increase the polymers' cationic charge, improving DNA binding affinity and condensation to formulate nanosized polyplexes, which highlights the critical role of terminal amines of LPAEs in DNA binding and condensation (*13*, *18*). Because of their highly branched structures, HPAEs contain multiple terminal amines (either primary or tertiary amines), which can thus significantly increase the positive charge of HPAEs, favoring DNA binding and condensation to form polyplexes through electrostatic interactions. Correspondingly, the high affinity enabled HPAEs to condense DNA into smaller polyplexes with relatively higher ζ potential (Fig. 2, E and F, and figs. S10, B and C, and S12).

TEM and AFM were used to investigate the difference in morphologies of polyplexes formulated by LPAEs or HPAEs with DNA. Representative TEM images and AFM images of the linear S5-B4-DATA/DNA and the corresponding highly branched S5-TMPTA-B4-DATA/DNA polyplexes are shown in fig. S13. It can be seen that both S5-TMPTA-B4-DATA/DNA and S5-B4-DATA/DNA manifest nano-ring morphologies; however, under water conditions, linear S5-B4-DATA/DNA polyplexes are more aggregated. Because of the branched structures, there are more amines with a positive charge at the terminals of HPAEs. The multiple terminal amines are present on the HPAE/DNA polyplex surface, potentially increasing the repulsive interaction between polyplexes; therefore, HPAE/DNA polyplexes were less aggregated compared to their LPAE/DNA counterparts. The same difference in polyplex aggregation was observed in the linear S4-BE-MPA/DNA and the corresponding highly branched S4-TMPTA-BE-MPA/DNA polyplexes (fig. S14). Previous reports have indicated that polyplex aggregation would potentially compromise polyplex cellular uptake efficiency and, ultimately, gene transfection efficiency (*1*).

Relative DNA binding ability, size, and ζ potential are key parameters that dictate polyplex cellular uptake efficiency. We hypothesized that branching could improve DNA binding and result in smaller polyplexes with higher ζ potential. The results showed that branching can indeed enhance polyplex cellular uptake (Fig. 2G and fig. S15A). After branching, the DNA binding of the linear S4-BE-MPA and S4-BGDA-MPA was increased by 30 to 50% (Fig. 2D), the corresponding highly branched S4-TMPTA-BE-MPA/DNA and S4-TMPTA-BGDA-MPA/DNA polyplexes have smaller sizes (100 to 300 nm) (Fig. 2E) and higher ζ potentials (12 to 25 mV) (Fig. 2F), and the cellular uptake efficiency was thus enhanced (8- to 22-fold) as quantified by flow cytometry, when compared to the corresponding linear S4-BE-MPA/DNA and S4-BE-MPA/DNA polyplexes (fig. S15, B and C). Because of the strong DNA binding, small size, and positive ζ potential, the linear S5-B4-DATA/DNA and S5-B4-E7/DNA polyplexes also exhibited high cellular uptake efficiency (fig. S15B). However, the fluorescence intensity of cells after treatment with the linear S5-B4-DATA/DNA and S5-B4-E7/DNA polyplexes was still lower than those treated with the corresponding highly branched S5-TMPTA-B4-DATA/DNA and S5-TMPTA-B4-E7/DNA polyplexes (fig. S15C). In comparison with other highly branched polyplexes, the S4 series, especially the highly branched S4-TMPTA-B6-MPA, S4-TMPTA-BE-MPA, and S4-TMPTA-BGDA-MPA, showed the highest increase in relative DNA binding and ζ potential, with a decrease in polyplex size; therefore, the cellular uptake and gene transfection efficiency of these polyplexes are enhanced most significantly (Fig. 2 and figs. S7 to S9).

Acid-base titrations were carried out to determine the proton buffering capacity of the linear S4-BE-MPA and the corresponding highly branched S4-TMPTA-BE-MPA. As shown in fig. S16A, the highly branched S4-TMPTA-BE-MPA exhibited stronger proton buffering capacity in the pH range of 5.0 to 7.4, which was made evident by a relatively flatter slope in the curve. The stronger proton buffering capacity of the highly branched S4-TMPTA-BE-MPA is possibly derived from the multiple terminal tertiary amines (morpholino groups). The highly branched S4-TMPTA-BE-MPA is deeper in color compared to the linear S4-BE-MPA because of the existence of more morpholino groups (fig. S16B). The main mechanism for effective endosomal escape of polyplexes formulated by LPAEs and DNA is due to the "proton sponge effect" (*13*, *37*). Therefore, the highly branched S4-TMPTA-BE-MPA showing stronger proton buffering capacity would potentially promote polyplex escape from endosomes. In addition, gel electrophoresis demonstrates that, in the presence of deoxyribonuclease, the highly branched S4-TMPTA-BE-MPA can more effectively protect DNA from degradation (fig. S11B), which further improves DNA delivery efficiency from endosomes. DNA binding affinity, polyplex size, ζ potential, and cellular uptake efficiency are related to the positive charge and proton buffering capacity of vectors. Branching can impart HPAEs with multiple terminal amine groups (either primary or tertiary), thus facilitating the multiple mechanistic steps involved in gene transfection and ultimately enhancing transfection efficiency. Note that gene transfection is an integrative process and is associated with multiple mechanistic steps (*1*, *3*). In addition to these mechanistic parameters, it cannot be excluded that other key steps may also be improved by the introduction of a branched structure and may ultimately enhance gene transfection synergistically (*1*, *5*, *35*).

Optimal HPAEs mediated potent gene transfection across diverse cell types

Because we aim to identify optimal HPAEs for broad use in gene transfection, the effect of various branched structures on transfection was further investigated. We chose to examine S4-TMPTA-BE-MPA in greater detail because it shows the strongest enhancement in gene transfection compared to the corresponding linear counterpart and thus would be the best candidate to explore the relationship between branched structure and gene transfection efficiency. Ten different versions of highly branched S4-TMPTA-BE-MPA were prepared by varying the B3/C2 feed ratio via the A2 + B3 + C2 synthesis platform (fig. S17 and table S9). Generally, as the feed ratio increased, the S4-TMPTA-BE–based polymer grew faster (figs. S18 and S19) and the residual vinyl groups [around 6.0 parts per million (ppm)] also increased (fig. S20). The vinyl groups were then functionalized with MPA by endcapping, and multiple functional morpholino groups were

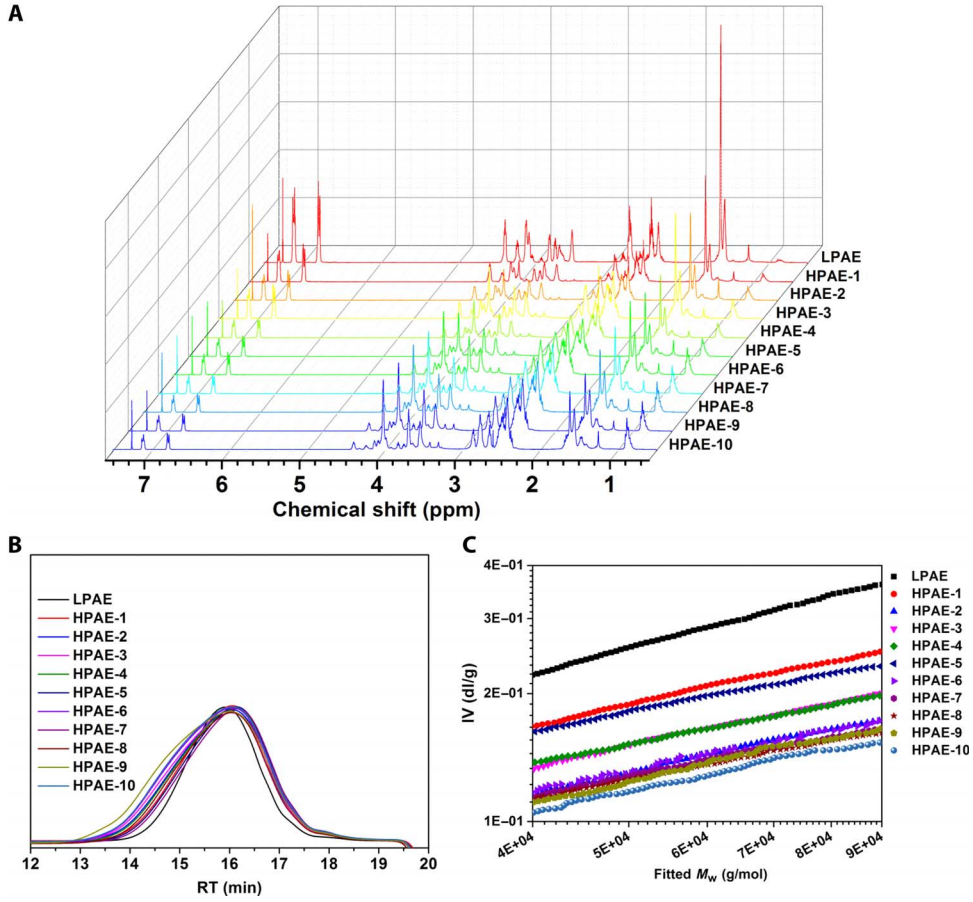

Fig. 3. Characterization of the highly branched S4-TMPTA-BE-MPA with different branched structures. (**A**) ^{1}H NMR spectra of the 10 versions of HPAEs and LPAE. As the feed ratio of TMPTA/BE increased, the TMPTA units in HPAEs increased, whereas the BE units decreased correspondingly. (**B**) GPC traces show that the HPAEs and LPAE have an M_w of around 12,000. (**C**) MH plots of the HPAEs and the corresponding LPAE. Increases in the feed ratio of TMPTA/BE resulted in a sequential decrease of α values of the LPAE and HPAEs. LPAE had an α value of 0.65, confirming its typical linear structure. In contrast, the α value of HPAEs decreased from 0.48 (HPAE-1) to 0.31 (HPAE-10), proving their highly branched structures. IV, intrinsic viscosity.

consistently introduced (Fig. 3A and figs. S21 and S22). The 10 versions of S4-TMPTA-BE-MPA had similar molecular weights (M_w ~ 12,000; Fig. 3B) and PDI values (around 2.2). The MH plot α values sequentially decreased from 0.48 for HPAE-1 to 0.31 for HPAE-10 (Fig. 3C). The monomer feed ratios correlate very well with the polymer composition and structure (table S10), further demonstrating the controllability and flexibility of the A2 + B3 + C2 strategy for branched polymer synthesis. Even with a very high B3/C2 feed ratio (>90% for HPAE-10), polymerization can still be effectively controlled and branched structures can be adjusted by simply varying the B3/C2 feed ratio.

Polyplex characterization parameters for the 10 HPAEs were similar; all of them showed strong DNA binding affinity of more than 75% (fig. S23A), translating the formation of positively charged and small HPAE/DNA polyplexes with an average diameter of 160 to 220 nm (fig. S23, B and C). The minute sizes imply the broad spectrum of targets and applications that HPAEs could exploit in a variety of tissues (*38*–*41*). In contrast, the corresponding LPAE exhibited lower DNA binding affinity, and the formulated LPAE/DNA polyplexes with negative surface charges were bigger in size.

Gene transfection efficiency and safety of the 10 HPAEs on HeLa cells were analyzed, as shown in fig. S24. The data sets clearly showed that, depending on their branched structure, the HPAEs exhibited 12- to 2400-fold higher Gluciferase activity than the LPAE, while maintaining more than 90% of the cell viability. Upon comparison with commercial transfection reagents (PEI, SuperFect, and Lipofectamine2000), HPAE-1, HPAE-2, HPAE-3, and HPAE-4 (with relatively lower branching) still mediated 5- to 20-fold enhancements in transfection efficiency. These results further support the fact that branching plays a critical role in improving the transfection potency of poly(β-amino ester)s. The fact that the 10 versions of HPAEs substantially differed in transfection efficiency indicates the necessity to optimize the branched structure of HPAEs via the A2 + B3 + C2 synthesis platform to ultimately identify the optimal candidates.

We wondered whether HPAEs had a sufficiently broad utility in gene transfection. To this end, a broad spectrum of 12 cell types was further tested. From the above gene transfection (fig. S24), it can be seen that HPAEs with low and medium degrees of branching are more efficient; therefore, HPAE-2 (with low branching) and HPAE-4 (with medium branching; Fig. 4) were chosen for the evaluations. On epithelial

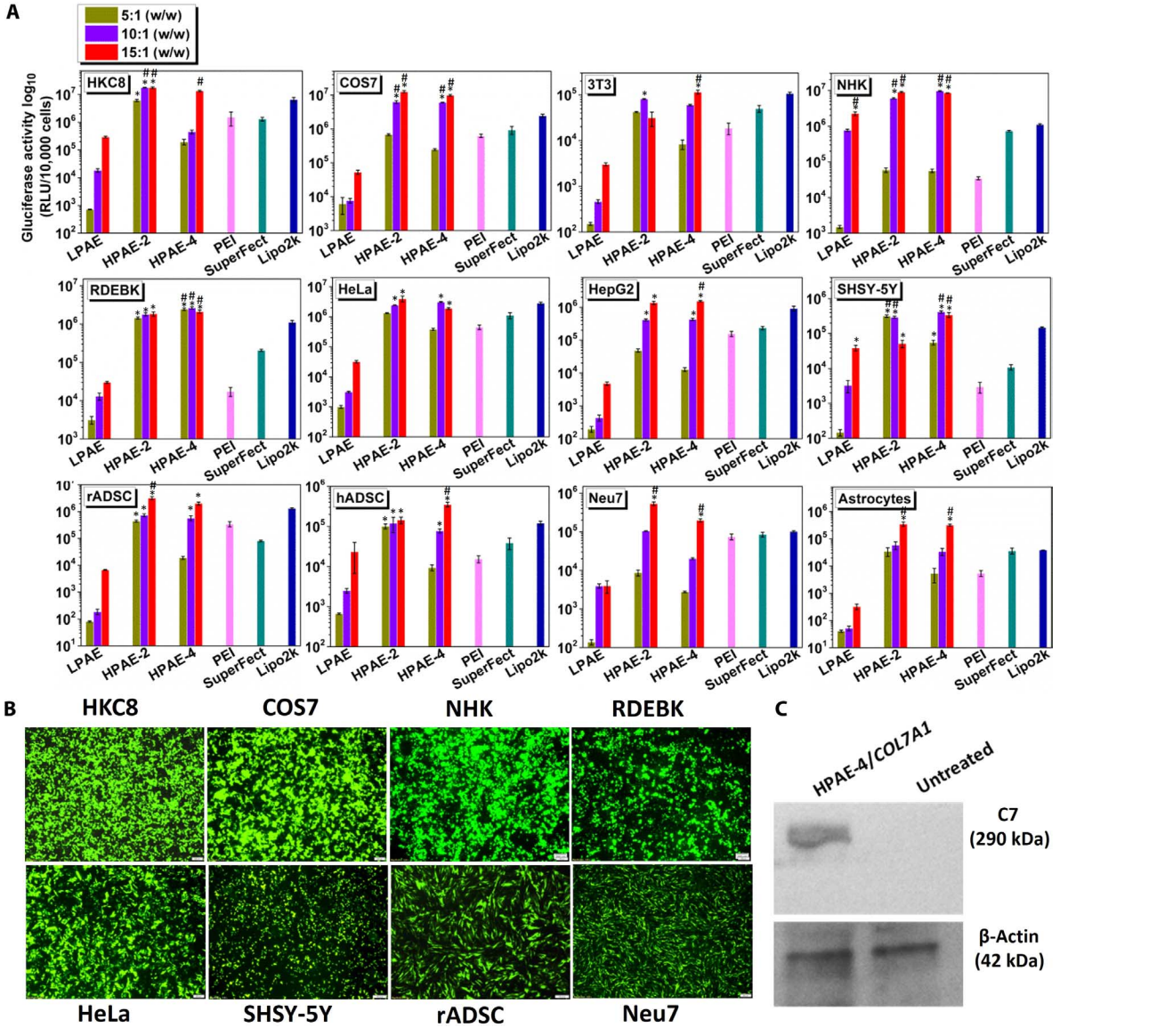

Fig. 4. HPAE-2 and HPAE-4 have broad utilities in gene transfection over diverse cell types. (**A**) Gluciferase activity of cells after treatment with HPAE-2 and HPAE-4 shows an up to 8521-fold enhancement compared to that mediated by the LPAE, PEI, SuperFect, and Lipofectamine 2000. One-way analysis of variance (ANOVA) was used; data are shown as average ± SD; $n = 4$. Data points marked with asterisks (*) are statistically significant relative to the SuperFect group, and data points marked with the pound sign (#) are statistically significant relative to the Lipofectamine 2000 group. *$P < 0.05$, superior Gluciferase activity compared with SuperFect; #$P < 0.05$, superior Gluciferase activity compared with Lipofectamine 2000. (**B**) Representative fluorescence images of cells after transfection with HPAE-4/DNA polyplexes at 15:1 (w/w). Scale bars, 200 μm. (**C**) Western blotting results from the supernatant of RDEBK cells. A clearly visible band for C7 was seen after transfection with HPAE-4/COL7A1.

cells (HKC8), fibroblasts (COS7 and 3T3), keratinocytes (NHK and RDEBK), and cancer cells (HeLa and HepG2), HPAE-2 and HPAE-4 mediated great transfection efficiency, especially at a ratio of 15:1 (w/w), and the Gluciferase activity was up to 8521-fold higher compared with that of the corresponding LPAE (Fig. 4A). It is well known that stem cells and astrocytes are particularly difficult to transfect (*11*). On rADSC, hADSC, SHSY-5Y astrocytes, Neu7 astrocytes, and primary astrocytes, the LPAE exhibited poor transfection efficiency, with Gluciferase activities one to two orders of magnitude lower than those of immortalized cells (for example, HKC8 and HeLa). In contrast, after treatment with HPAE-2 and HPAE-4, the Gluciferase activity of these stem cells and astrocytes remained very high and even close to that of immortalized cells, highlighting the fact that the HPAEs can mediate high gene transfection regardless of cell phenotypes. The superior transfection potency of HPAEs after transfection was also quantitated by the expression of GFP using flow cytometry (fig. S25). On HKC8, COS7, NHK, RDEBK, HeLa, and rADSC, more than 75% of the cells became GFP-positive after treatment by HPAE-2 and HPAE-4 (on HKC8, up to 98% became GFP-positive), which is a significant improvement compared with the less than 10% transfection efficiency mediated by the

LPAE (except for the 34.82% achieved on the RDEBK). In the most challenging hADSC and primary astrocytes, HPAE-2 and HPAE-4 also showed more than 35% transfection efficiency compared with the negligible transfection efficiency mediated by the corresponding LPAE. Representative images of cells after transfection are shown in Fig. 4B. The superior transfection potency of HPAEs was further supported by a Western blotting assay using the COL7A1 DNA coding C7 (Fig. 4C). The fact that it can effectively deliver COL7A1 into the C7-null RDEBK cells to mediate the recombinant C7 production indicates the potential of HPAE-4 for therapeutic use in vivo. Together, the results from the Gluciferase assays, flow cytometry measurements, and Western blotting assays substantiate the fact that branching can significantly enhance the gene transfection potency of poly(β-amino ester)s and the fact that LPAEs, even with poor transfection efficiency (for example, S4-BE-MPA), could be upgraded to potent vectors by proper branching (for example, S4-TMPTA-BE-MPA). Note that, in this context, the 12 cell types tested were obtained from various tissues with different phenotypes; thus, the fact that HPAEs showed superior transfection efficiency on all of them suggests great potential for their use across many clinical targets. Also note that the high transfection efficiency of the HPAEs was achieved at much lower w/w ratios (5:1, 10:1, and 15:1), in contrast with the w/w ratio of equal to or greater than 20:1 for the LPAEs in previous reports (*40*–*42*), which further highlights the superiority of HPAEs in gene transfection. In addition, HPAEs can maintain high cell viability even in stem cells and astrocytes (fig. S26).

Optimal HPAE mediated long-term recombinant protein expression in vivo

Although many gene vectors show high levels of reporter gene expression in vitro, the translation of such success to yield the expression of a recombinant protein in vivo, especially in terms of persistency, is far more challenging (*37*–*45*). Hence, the effectiveness of optimal HPAEs was further assessed using a human RDEB graft mouse model. RDEB is a devastating and debilitating genetic skin disorder, characterized by chronic fragility and blistering of the skin and mucosal membranes caused by mutations in the COL7A1 gene, which encodes for the C7 protein, a key component of anchoring fibrils that serves to secure the attachment of epidermis to the dermis (*38*). The C7 protein is secreted from cells to localize along the base membrane zoon (BMZ). Absence of C7 results in growth retardation and the formation of blisters (*46*). To date, there is no effective therapy, and this highlights the fact that our use of the human RDEB model to assess the effectiveness of the HPAEs has both scientific and clinical significance (*47*). The most widely used technique to detect C7 expression in vivo is immunofluorescence staining (*48*, *49*).

The superior transfection efficiency of HPAE-4 across various cell types makes it an ideal vector for delivering COL7A1 coding sequences to restore the expression of C7 in vivo. HPAE-4 carrying the COL7A1 coding sequences for human C7, termed HPAE-4/COL7A1 polyplexes [15:1 (w/w)], was directly injected into the dermis of the human RDEB graft sites (n = 4). A regime of three injections, once every other day, was applied to all the grafts. At days 5 and 30 from the last injection, two mice were sacrificed by CO_2 asphyxiation. Tissues were harvested and immunofluorescence staining was used to detect the production of C7. When stained by the mouse monoclonal LH7.2 antibody and rabbit polyclonal antibody, the tissues from day 5 are clearly seen to be positive for recombinant C7, with significant levels of C7 produced and highly localized along the BMZ (Fig. 5C). After 30 days, C7 persisted to a native level of protein and extended for the full length of the human RDEB grafts (Fig. 5D). Immunohistochemical staining was further used to assess the structure of the skin tissue, demonstrating that the tissues subjected to three injections appeared normal in structure and human graft stratification (fig. S27). These results provide convincing evidence for the potential and feasibility of HPAE-4 to mediate C7 expression in human RDEB, especially given the long-term C7 expression.

DISCUSSION

Gene therapy has been considered one of the most promising modes of treatment because almost all diseases have a genetic component (*8*). Unfortunately, the translation of gene therapy from bench to bedside is predominantly hindered by the lack of clinically viable vectors, which ideally not only can mediate potent transfection efficiency but also can induce minimal cytotoxicity (*3*). In the past two decades, tremendous efforts have been dedicated to this significant challenge, including the development of structurally diverse liposomes, cationic polymers, peptides, and inorganic nanoparticles, among others (*13*). However, although considerable progress has been made, the improvement in potency is usually at the expense of safety, and in vivo results generally do not correlate well with in vitro data (*7*, *44*, *45*). The latter finding is particularly true when comparing a therapeutic gene to a reporter gene. In 2000, Lynn *et al.* (*13*) reported their pioneer work on developing poly(β-amino ester)s, which were synthesized through conjugated addition of amines to diacrylates. Later on, Anderson *et al.* (*15*) developed a high-throughput technique for the rapid synthesis and screening of structurally diverse libraries of LPAEs.

Successful gene transfection critically depends on the condensation of DNA by the vector to formulate high-performing polyplexes. In general, polyplexes of smaller size and higher ζ potential are more favorable for cellular uptake. Polyplexes with higher proton buffering capacity have stronger endosomal escape ability. All these beneficial characteristics are related to the vector's topological structure (for example, linear or branched). Previous reports have demonstrated that branched PEI, PLL, and PDMAEMA are more efficient in gene transfection than their corresponding linear counterparts (*4*, *24*–*26*). Therefore, we believe that the potential of poly(β-amino ester)s has not yet been fully exploited because, to date, only LPAEs have been developed. Given the limitations of a linear structure (for example, only two terminal groups) (*3*), we hypothesize that transfection efficiencies may greatly benefit from the development of dendritic or branched poly(β-amino ester)s through expansion of their molecular structure from linear to 3D. However, the existing approaches for branched polymer synthesis usually require special monomer systems, and the controllability in polymerization is also very challenging (*34*). To address these issues, in our previous work, we developed two HPAEs via the A2 + B3 + C2 Michael addition using a specific monomer combination and showed the high efficiency of HPAEs regarding the transfection of keratinocytes, especially when a minicircle DNA was used (*50*). Encouraged by these results, we aim to find answers for the following questions: (i) How generalizable is the A2 + B3 + C2 synthesis strategy (in terms of controllability and flexibility) and can this synthesis strategy be expanded to a broader library of monomer combinations? (ii) Would the branching degree have significant effects on the gene transfection efficiency and safety of HPAEs? (iii) How broad is the applicability of HPAEs regarding the transfection

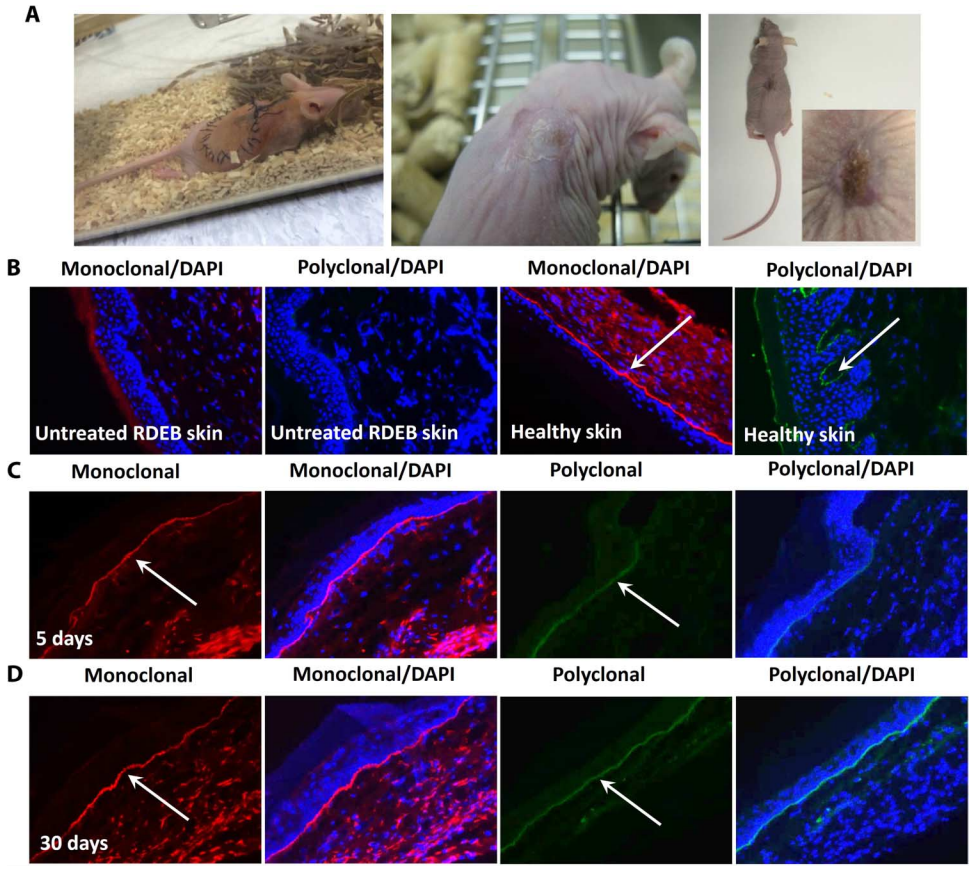

Fig. 5. HPAE-4 mediates a long-term expression of C7 in a human RDEB graft mouse model. (**A**) Human RDEB grafts 0 day (left), 21 days (middle), and 60 days (right) after surgery. (**B**) Immunofluorescence image clearly shows the band of C7 along the BMZ (indicated by arrows) in the "healthy" skin graft. DAPI, 4′,6-diamidino-2-phenylindole. (**C**) Five days after the last injection of the HPAE-4/COL7A1 polyplexes, a significant level of C7 was produced and localized along the BMZ (indicated by the arrows). (**D**) After 30 days, the level of C7 along the BMZ remained at a significant level (indicated by the arrows).

of diverse cell types, especially difficult-to-transfect cell types (for example, stem cells and astrocytes)? (iv) What are the possible mechanisms behind the enhancement in gene transfection efficiency compared to the LPAEs? (v) How would the optimal HPAE perform in vivo? Therefore, in this work, we report the general applicability of the platform for branched polymer synthesis based on the unique A2 + B3 + C2 branching strategy.

It can be clearly noticed that on HeLa, rADSC, and SHSY-5Y cells, HPAEs always mediated higher gene transfection compared to the corresponding LPAEs, including the best-performing linear C32 series. Follow-up investigations into the underlying mechanisms showed that branching can improve DNA binding, condensation, protection, proton buffering capacity, and polyplex cellular uptake, which are the key steps that have been repeatedly reported in the literature for their crucial roles in gene transfection (*18*). To examine the broad utility of the transfection agents, we further optimized the representative S4-TMPTA-BE-MPA by adjusting the branched structure. The optimal HPAE-2 and HPAE-4 mediated a highly efficacious gene transfection across 12 cell types, including stem cells and primary cells. Finally, we evaluated the effectiveness of the application of HPAE in vivo. We used a human RDEB graft murine model to introduce HPAE-4/COL7A1 polyplexes into the human RDEB graft skin. Significant levels of recombinant C7 expression were detected 5 days after polyplex injections. After 30 days, the remaining recombinant protein was still at a significant level. Because of the higher fragility of human RDEB skin (*48*), these results have a huge significance because the animal model used here was very close to the ultimate clinical application situation. Furthermore, the long-term recombinant protein expression can substantially reduce the frequency of administration and thus reduce the overall cost of treatment. The promising in vitro and in vivo results not only demonstrate that branching can significantly enhance the gene transfection efficiency of poly(β-amino ester)s but also reveal the potential promise of HPAEs in clinical applications.

MATERIALS AND METHODS

Polymer synthesis and characterization

Three groups of HPAEs were synthesized. In group 1, diacrylates in the sets of monomers (table S1) were varied. Monomers were first dissolved in DMSO (500 mg/ml), and then the required volumes of monomer solutions were added into a glass vial according to feed

ratios (table S2). The reaction occurred at 90°C. Termination of the polymerization was achieved by diluting the base polymers to 100 mg/ml with DMSO and then endcapping with a second amine at room temperature for 48 hours. The final polymer products were purified by precipitation in diethyl ether three times and then dried under vacuum for 24 hours before being stored at −20°C for subsequent studies. In group 2 (tables S1 and S2), the endcapping amines were varied systematically, and the polymers were synthesized and purified as above. In group 3 (table S9), the feed ratio of B3/C2 was varied sequentially, and polymers were synthesized and purified as above. To synthesize the corresponding LPAEs (tables S3 and S4), amines and diacrylates were directly mixed without solvent at 90°C (*13*, *15*). The reaction was terminated, and the final product was purified and stored as described above.

Molecular weights (M_w and M_n) and PDI values of the HPAEs and corresponding LPAEs were measured by GPC. Base polymers in group 1 and group 2 were analyzed using an Agilent 1260 Infinity GPC system with a refractive index detector. GPC columns (ResiPore, 250 mm × 4.6 mm; two in series) were eluted with *N*,*N*′-dimethylformamide (DMF) and 0.1% LiBr at a flow rate of 0.67 ml/min at 80°C. Base polymers in group 3 were analyzed using an Agilent 1260 Infinity GPC system equipped with a refractive index detector, a viscometer detector, and a dual-angle light-scattering detector (LS 15° and LS 90°). GPC columns (PolarGel-M, 7.5 mm × 300 mm; two in series) were eluted with DMF and 0.1% LiBr at a flow rate of 1 ml/min at 60°C. GPC columns were calibrated with linear poly(methyl methacrylate) standards. To analyze the molecular weights of the base polymers, 20 μl of the reaction solution was taken at different time points, diluted with 1 ml of DMF, filtered through a 0.2-μm filter, and then measured by GPC. To analyze the final polymer products, 10-mg samples were dissolved in 2 ml of DMF, filtered through a 0.2-μm filter, and then measured by the GPC with triple detectors. The chemical structure and composition of the polymers were confirmed with NMR. Polymer samples were dissolved in $CDCl_3$, and ^1H NMR spectra were obtained on a Varian Inova 400-MHz spectrometer and reported in parts per million, relative to the response of the solvent (7.24 ppm) or to tetramethylsilane (0.00 ppm). ^{13}C NMR spectra were carried out at 150 MHz and reported in parts per million, relative to the response of the solvent (77.2 ppm). Proton buffering capacities of the linear S4-BE-MPA and the corresponding S4-TMPTA-BE-MPA were determined with acid-base titration. The linear S4-BE-MPA or the highly branched S4-TMPTA-BE-MPA (10 mg) DMSO stock solution (100 mg/ml) was diluted in 10 ml of distilled water. The initial pH value was set to 3.0 using 0.1 M HCl and then titrated to pH 10.0 using NaOH (0.01 M). The pH values were measured using a Sartorius PB-10 pH meter with 100-μl increments.

Polyplex characterization

To measure the DNA binding affinity of the HPAEs and the corresponding LPAEs, PicoGreen assays were used according to a previous report (*11*). Briefly, polymers were initially dissolved in DMSO to give stock solutions (100 mg/ml). According to the w/w ratio, polymer and DNA (2 μg for each sample) were diluted with 30 μl of sodium acetate buffer (pH 5.2 ± 0.1; 0.025 M), mixed by vortex for 10 s, and allowed to incubate for 10 min. Sixty microliters of the PicoGreen solution (80 μl of PicoGreen diluted with 15.92 ml of sodium acetate buffer) was added and allowed to incubate for another 5 min. In a black 96-well plate, 200 μl of Dulbecco's modified Eagle's medium was added, and then 30 μl of the polyplex/PicoGreen solution was added. Fluorescence was measured with a plate reader with an excitation at 490 nm and an emission at 535 nm. The DNA condensation ability of the linear S4-BE-MPA and the corresponding highly branched S4-TMPTA-BE-MPA was determined with gel electrophoresis. DNA (1 μg) was used for each sample preparation. Briefly, the linear S4-BE-MPA and the highly branched S4-TMPTA-BE-MPA were initially dissolved in DMSO to stock solutions (100 mg/ml), and then the stock solutions were further diluted with sodium acetate buffer (pH 5.2; 0.025 M) according to the w/w ratio (ranging from 10:1 to 50:1). DNA was diluted to 0.1 mg/ml with sodium acetate buffer. The linear S4-BE-MPA and the highly branched S4-TMPTA-BE-MPA solutions were added into the DNA solution, vortexed for 10 to 15 s, and allowed to stand for 10 to 15 min. Polyplexes were then loaded into the wells of 1% agarose gel, and electrophoresis was conducted at 120 V for 40 min. To investigate the DNA protection ability of the linear S4-BE-MPA and the highly branched S4-TMPTA-BE-MPA, polyplexes were prepared as mentioned above, $MgCl_2$ (2.5 mM final concentration) and deoxyribonuclease I (2 USP units of pDNA per milligram) were added, and polyplexes were incubated at 37°C for 30 min. Afterward, the enzyme reaction was stopped by adding EDTA (25 mM final concentration). Gel electrophoresis was then carried out as above. To measure polyplex sizes and ζ potentials, DNA (2 μg for each sample) was diluted in sodium acetate buffer. According to the w/w ratio, the polymer was also diluted with sodium acetate buffer, mixed with DNA solution by vortex for 10 s, and then allowed to incubate for 10 min. Polyplexes were then diluted with phosphate-buffered saline (PBS) to 1 ml. A Malvern Instruments Zetasizer (Nano-2590) with a scattering angle of 150° was used to measure polyplex sizes and ζ potentials. All experiments were repeated at a minimum of four times.

The morphological structures of the linear S5-B4-DATA/DNA and the corresponding highly branched S5-TMPTA-B4-DATA/DNA polyplexes were investigated with TEM. Polyplexes were prepared as before. Polyplex solution (10 μl) was applied to holey carbon films on 200-mesh copper grids and dried in air for 2 hours. The copper grids were then washed with deionized water to remove the crystals of buffer salts. Samples were stained with uranium acetate (0.5%) for 2 min. TEM (FEI Tecnai 120) was carried out at 120 kV at the University College Dublin Conway Core Technology Center. To investigate the morphology of polyplexes with AFM, the linear S5-B4-DATA/DNA and S4-BE-MPA/DNA polyplexes and the corresponding highly branched S5-TMPTA-B4-DATA/DNA and S4-TMPTA-BE-MPA/DNA polyplexes were prepared as mentioned above. Twenty-five microliters of polyplexes suspension in sodium acetate buffer was dropped onto a freshly cleaved mica substrate and incubated for 2 min, after which the excess polyplex solution was removed by N_2 flow. The surface was flushed with 200 μl of distilled water three times, and then 200 μl of distilled water was dropped on the surface. AFM images of the polyplexes were acquired in water using Asylum Research MFP-3D AFM. Scans were conducted in amplitude modulation mode with Nanosensors PPP-NCHR cantilevers having a nominal force constant of 42 N/m, a resonance frequency of 330 kHz, and a typical tip radius of less than 7 nm. Image processing and height profile analysis were performed using Asylum software (IGOR Pro, WaveMetrics).

In vitro transfection

For in vitro transfections using Gluciferase DNA, cells were seeded on 96-well plates at a density of 1×10^4 to 2×10^4 cells per well in 100 μl of medium and cultured until 70 to 80% confluent. The stem cells (rADSC and hADSC) used for transfecting were below passage 4,

and the primary astrocytes and SHSY-5Y used for transfection were under passage 5. Before transfection, we optimized the commercial transfection reagents SuperFect, PEI, and Lipofectamine 2000 according to the manufacturer's instructions and we referred to previous publications as well (*4*, *12*, *51*). To optimize these reagents, GFP was used as a reporter gene and DNA dosage (ranging from 0.1 to 1 μg per well of 96-well plates and from 1 to 5 μg per well of 24-well plates) and the ratios of reagent to DNA (ranging from 1:1 to 10:1 for PEI, from 2:1 to 10:1 for SuperFect, and from 1:1 to 5:1 for Lipofectamine 2000) were systematically varied. Forty-eight hours after transfection, we observed and compared GFP expression and cell morphologies using a fluorescence microscope to find the optimal conditions for transfection. All transfections with the commercial reagents were thus carried out with our optimized formulations: SuperFect, 9:1 (w/w); PEI, 3:1 (w/w); Lipofectamine 2000, 3:1 (w/w). To compare the gene transfection efficiency of HPAEs with the corresponding LPAEs (group 1 and group 2; tables S1 and S3), HeLa, rADSC, and SHSY-5Y were used with 0.25 μg of DNA per well at 20:1 and 50:1 (w/w), respectively [Green *et al.* (*13*) and Eltoukhy *et al.* (*17*) have previously demonstrated that optimal formulations for efficient gene transfection of LPAEs usually tend to have w/w ratios greater than 20:1; therefore, 20:1 and 50:1 (w/w) were chosen to evaluate the gene transfection efficiency of various HPAEs and corresponding LPAEs]. To compare the gene transfection efficiency of the 10 different versions of the highly branched S4-TMPTA-BE-MPA (group 3; table S9) in HeLa cells, 0.25 μg of DNA was added per well at 10:1 (w/w). For all other transfections with Gluciferase, 0.25 μg of DNA was used for primary and stem cells and 0.5 μg of DNA was used for immortalized cells at 5:1, 10:1, and 15:1 (w/w). Before the transfection, polyplexes were prepared. Briefly, linear LPAEs and highly branched HPAEs were initially dissolved in DMSO to stock solutions (100 mg/ml), and then the stock solutions were further diluted with sodium acetate buffer according to the w/w ratio. DNA was diluted to 0.1 mg/ml with sodium acetate buffer. LPAEs or HPAE solutions were added into the DNA solution, vortexed for 10 to 15 s, and allowed to stand for 10 to 15 min. The cell culture medium was then added to increase the volume of the polyplex solution to 100 μl. The medium in the wells of cell culture plates was removed quickly, and the polyplex solution was added. After 4 hours, the medium was replaced with 100 μl of fresh medium, and the cells were cultured for another 44 hours. Control cells were subjected to the same treatment but incubated only with DNA or with comparative controls for the commercial transfection reagents PEI, SuperFect, and Lipofectamine 2000. Analysis of the secreted Gluciferase activity was performed as per the provided protocol, with Gluciferase activity directly detected in the cell supernatant and plotted in terms of relative light units. Cytotoxicity analysis was performed on all cells using the Alamarblue reduction method. To perform this assay, cell supernatants were initially removed and then cells were washed with Hank's balanced salt solution (HBSS), followed by the addition of 10% Alamarblue in HBSS. Living, proliferating cells maintain a reducing environment within the cytosol of the cell, which acts to reduce the active, nonfluorescent ingredient (resazurin) in Alamarblue to the highly fluorescent compound, resorufin. This reduction brings about a color change from blue to light red and allows the quantitative measurement of cell viability based on the increase in overall fluorescence and color of the medium. The Alamarblue solution from each well was transferred to a fresh flat-bottomed 96-well plate for fluorescence measurements at 590 nm. Control cells without polyplex treatment were used to normalize the fluorescence values and plotted as 100% viable. All Gluciferase and Alamarblue reduction experiments were performed in quadruplicate with the margin of error shown as ±SD. For in vitro transfections using GFP DNA, cells were seeded in 24-well plates at a density of 5×10^4 to 1×10^5 cells per well in 500 μl of medium. Transfections were conducted as mentioned above, but 1 μg of DNA per well was used for primary cells and stem cells and 2 μg of DNA per well was used for immortalized cells. For flow cytometry measurements, after transfection, cells were collected as per standard cell culture protocols, and propidium iodide was used to exclude the dead cells. To visualize the transfected cells with a fluorescence microscope, 48 hours after transfection, the medium was removed and cells were washed in HBSS three times and then visualized under a fluorescence microscope (Olympus IX81).

Polyplex cellular uptake

GFP DNA was labeled with a Cy3 (a red fluorescent dye) labeling kit as per the recommended protocol. In 96-well plates, HeLa cells were seeded at 5000 cells per well. Gene transfection was conducted as above with 0.1 μg of DNA per well at a ratio of 20:1 (w/w). After 4 hours, the medium was removed and cells were fixed with 4% paraformaldehyde after washing with PBS for three times. Next, the cells were permeabilized with 0.1% Triton X-100 and stained with DAPI, followed by visualization under a fluorescence microscope (Olympus IX81). To quantify polyplex cellular uptake efficiency, gene transfection was carried out in 24-well plates (20,000 cells per well) with 0.5 μg of DNA per well at a ratio of 20:1 (w/w). After 4 hours, cells were collected according to standard protocols, and the polyplex cellular uptake efficiency was analyzed using flow cytometry.

Western blot assay

RDEBK cells were seeded in a T175 flask 24 hours before transfection. HPAE-4/COL7A1 polyplexes (60 μg of DNA) were prepared as mentioned above and added into the wells. After 48 hours, the supernatant was harvested, concentrated, and denatured following standard protocols. The protein solution was loaded into the SDS–polyacrylamide gel electrophoresis gel (6%) and run at 130 V for 70 min and then at 100 V for 15 min. Next, the protein sample was transferred onto a nitrocellulose membrane at 80 V for 1 hour. Membrane blocking was performed for 1 hour at room temperature using 5% bovine serum albumin TBS-T (tris-buffered saline with Tween 20) buffer. Protein sample underwent overnight incubation at 4°C in a primary antibody (C7 antibody) diluted in 5% blocking buffer. The membrane was washed three times in TBS-T (5 min each). Following washes, the protein sample was incubated with a secondary antibody (anti-rabbit horseradish peroxidase) in 5% blocking buffer for 1 hour at room temperature. Finally, the membrane was washed three times in TBS-T. Images were gathered using standard darkroom development techniques for chemiluminescence.

Evaluation of HPAE-4/COL7A1 polyplexes with a human RDEB graft mouse model

Full permission for the RDEB murine model was granted to the Centro de Investigaciones Energéticas Medioambientales y Tecnológicas (CIEMAT)–Centro de Investigación Biomédica en Red de Enfermedades Raras (CIBERER-U714) with Spanish registration number 28079-21 A and European registration number ES280790000183. The primary cells that express C7 used in this study were obtained from the Spanish Blood and Tissue Bank (Centro Comunitario de Sangre y Tejidos), which complies with the European Tissues and Cells Directive 2004/23/EC of the European Parliament and of the Council of 31 March 2004.

The human RDEB graft mouse model was produced according to previous reports (*52*–*54*). The human RDEB skin equivalents were produced with primary fibroblasts and keratinocytes from different patients but both with the same homozygous mutation in COL7A1. In total, six mice (nude, female, 7 weeks old) were grafted successfully, of which five were grafted with RDEB skin equivalents and one was grafted with "healthy" skin equivalents. The healthy skin equivalent was harvested for use as a positive control for immunostaining. Four of the five human RDEB grafts were subjected to intradermal injections (once every other day) of HPAE-4/COL7A1 polyplexes three times; the other one was left untreated as a negative control. Injections were performed after general anesthesia, and the mice remained unconscious for an additional 30 min. Polyplexes were prepared by mixing HPAE-4 with COL7A1 at high concentration [20 μg of COL7A1, 15:1 (w/w); the total volume of the polyplex solution was 50 μl], and then they were directly injected into the dermis of the human RDEB graft sites. Tissue samples were harvested 5 and 30 days after the last injection. The animals were sacrificed by CO_2 asphyxiation, and the skin tissues were harvested. The tissues were fixed in paraformaldehyde or frozen for antibody staining. Monoclonal mouse antibody LH7.2 and polyclonal rabbit antibody were used to stain for human C7. Immunofluorescence images were taken from different areas of BMZ. To confirm that the tissues were human, the epidermis and the dermis were stained with the human-specific antibodies involucrin and vimentin (BioGenex), respectively. Formaldehyde-fixed paraffin tissue samples and a peroxidase secondary antibody (Jackson) were used for both epidermis and dermis. Once the proteins were stained, the tissue was further stained with hematoxylin to visualize the structure.

Statistics

All transfection data were analyzed using GraphPad Prism version 5 (GraphPad Software). D'Agostino and Pearson omnibus normality tests were used to determine normal distribution. Where normal distribution was evident, a one-way ANOVA was performed, followed by Tukey's post hoc test. P values < 0.05 were considered to be statistically significant. All transfection experiments were performed in quadruplicate unless otherwise stated, with error bars indicating ±SD.

SUPPLEMENTARY MATERIALS

Supplementary material for this article is available at http://advances.sciencemag.org/cgi/content/full/2/6/e1600102/DC1

Experimental procedure

fig. S1. GPC traces of HPAE base polymers.

fig. S2. GPC traces of LPAE base polymers.

fig. S3. GPC traces of HPAEs.

fig. S4. GPC traces of LPAEs.

fig. S5. MH plots of HPAEs and the corresponding LPAEs.

fig. S6. Comparison of ^{1}H NMR spectra of HPAEs with the corresponding LPAEs.

fig. S7. Gluciferase activity of HeLa, rADSC, and SHSY-5Y after treatment with various HPAEs and corresponding LPAEs at 50:1 (w/w).

fig. S8. Representative GFP images of cells after treatment with HPAEs and the corresponding LPAEs.

fig. S9. Cell viability of HeLa cells, rADSC cells, and SHSY-5Y cells after treatment with HPAEs and the corresponding LPAEs at 20:1 and 50:1 (w/w).

fig. S10. Characterization and comparison of polyplexes formulated from HPAEs or the corresponding LPAEs with DNA at 50:1 (w/w).

fig. S11. DNA condensation and protection ability of the highly branched S4-TMPT-BE-MPA and the corresponding linear counterpart S4-BE-MPA.

fig. S12. Size distribution of polyplexes formulated by HPAEs or the corresponding LPAEs with DNA at 20:1 (w/w).

fig. S13. Morphological characterization of the linear S5-B4-DATA/DNA and the corresponding highly branched S5-TMPTA-B4-DATA/DNA polyplexes with TEM and AFM.

fig. S14. AFM height images of the linear S4-BE-MPA/DNA and the corresponding highly branched S4-TMPTA-BE-MPA/DNA polyplexes in water.

fig. S15. Comparison of cellular uptake efficiency of polyplexes formulated by HPAEs or the corresponding LPAEs with Cy3-labeled DNA at 20:1 (w/w).

fig. S16. Proton buffering capacity of the linear S4-BE-MPA/DNA and the corresponding highly branched S4-TMPTA-BE/DNA polyplexes.

fig. S17. Synthesis of S4-TMPTA-BE-MPA of different branched structures via the A2 + B3 + C2 Michael addition approach.

fig. S18. GPC traces of HPAE base polymers of varying TMPTA/BE feed ratios.

fig. S19. GPC traces of HPAE base polymers before endcapping.

fig. S20. ^{1}H NMR spectra of HPAE and the corresponding LPAE base polymers.

fig. S21. HPAE ^{1}H NMR and the corresponding ^{13}C NMR spectra.

fig. S22. LPAE ^{1}H NMR and the corresponding ^{13}C NMR spectra.

fig. S23. Characterization of polyplexes formulated by the 10 versions of S4-TMPTA-BE-MPA and DNA.

fig. S24. Evaluation of the gene transfection efficiency and cytotoxicity of the 10 versions of S4-TMPTA-BE-MPA.

fig. S25. Transfection efficiency of HPAE-2, HPAE-4, LPAE, and commercial transfection reagents in diverse cell types quantified by flow cytometry.

fig. S26. Cell viability after transfection with HPAE-2, HPAE-4, LPAE, and commercial reagents measured using Alamarblue assay.

fig. S27. Structure of the skin tissue assessed by immunohistochemical staining.

table S1. Sets of monomers for HPAE syntheses.

table S2. Monomer feed ratios for HPAE syntheses.

table S3. Sets of monomers for LPAE syntheses.

table S4. Monomer feed ratios for LPAE syntheses.

table S5. GPC results of HPAE base polymers.

table S6. GPC results of LPAE base polymers.

table S7. GPC results of HPAEs.

table S8. GPC results of LPAEs.

table S9. Monomer feed ratios for the synthesis of S4-TMPTA-BE-MPA of various branched structures.

table S10. Monomer feed ratios, polymer compositions, and structural information of S4-TMPTA-BE-MPA of different branched structures.

REFERENCES AND NOTES

1. D. W. Pack, A. S. Hoffman, S. Pun, P. S. Stayton, Design and development of polymers for gene delivery. *Nat. Rev. Drug Discov.* **4**, 581–593 (2005).
2. J. E. Dahlman, C. Barnes, O. F. Khan, A. Thiriot, S. Jhunjunwala, T. E. Shaw, Y. Xing, H. B. Sager, G. Sahay, L. Speciner, A. Bader, R. L. Bogorad, H. Yin, T. Racie, Y. Dong, S. Jiang, D. Seedorf, A. Dave, K. Singh Sandhu, M. J. Webber, T. Novobrantseva, V. M. Ruda, A. K. R. Lytton-Jean, C. G. Levins, B. Kalish, D. K. Mudge, M. Perez, L. Abezgauz, P. Dutta, L. Smith, K. Charisse, M. W. Kieran, K. Fitzgerald, M. Nahrendorf, D. Danino, R. M. Tuder, U. H. von Adrian, A. Akinc, D. Panigrahy, A. Schroeder, V. Koteliansky, R. Langer, D. G. Anderson, In vivo endothelial siRNA delivery using polymeric nanoparticles with low molecular weight. *Nat. Nanotechnol.* **9**, 648–655 (2014).
3. M. A. Minter, E. E. Simanek, Nonviral vectors for gene delivery. *Chem. Rev.* **109**, 259–302 (2009).
4. T. Zhao, H. Zhang, B. Newland, A. Aied, D. Zhou, W. Wang, Significance of branching for transfection: Synthesis of highly branched degradable functional poly(dimethylaminoethyl methacrylate) by vinyl oligomer combination. *Angew. Chem. Int. Ed. Engl.* **53**, 6095–6100 (2014).
5. D. Luo, M. Saltzman, Synthetic DNA delivery systems. *Nat. Biotechnol.* **18**, 33–37 (2000).
6. X. Guo, L. Huang, Recent advances in nonviral vectors for gene delivery. *Acc. Chem. Res.* **45**, 971–979 (2012).
7. J.-P. Behr, Synthetic gene transfer vectors II: Back to the future. *Acc. Chem. Res.* **45**, 980–984 (2012).
8. A. Akinc, A. Zumbuehl, M. Goldberg, E. S. Leshchiner, V. Busini, N. Hossain, S. A. Bacallado, D. N. Nguyen, J. Fuller, R. Alvarez, A. Borodovsky, T. Borland, R. Constien, A. de Fougerolles, J. R. Dorkin, K. Narayanannair Jayaprakash, M. Jayaraman, M. John, V. Koteliansky, M. Manoharan, L. Nechev, J. Qin, T. Racie, D. Raitcheva, K. G. Rajeev, D. W. Y. Sah, J. Soutschek, I. Toudjarska, H.-P. Vornlocher, T. S. Zimmermann, R. Langer, D. G. Anderson, A combinatorial library of lipid-like materials for delivery of RNAi therapeutics. *Nat. Biotechnol.* **26**, 561–569 (2008).
9. M. E. Davis, J. E. Zuckerman, C. H. J. Choi, D. Seligson, A. Tolcher, C. A. Alabi, Y. Yen, J. D. Heidel, A. Ribas, Evidence of RNAi in humans from systemically administered siRNA via targeted nanoparticles. *Nature* **464**, 1067–1070 (2010).

10. H. Wei, J. G. Schellinger, D. S. H. Chu, S. H. Pun, Neuron-targeted copolymers with sheddable shielding blocks synthesized using a reducible, RAFT-ATRP double-head agent. *J. Am. Chem. Soc.* **134**, 16554–16557 (2012).
11. A. Sizovs, L. Xue, Z. P. Tolstyka, N. P. Ingle, Y. Wu, M. Cortez, T. M. Reineke, Poly(trehalose): Sugar-coated nanocomplexes promote stabilization and effective polyplex-mediated siRNA delivery. *J. Am. Chem. Soc.* **135**, 15417–15424 (2013).
12. B. Newland, Y. Zheng, Y. Jin, M. Abu-Rub, H. Cao, W. Wang, A. Pandit, Single cyclized molecule versus single branched molecule: A simple and efficient 3D "knot" polymer structure for nonviral gene delivery. *J. Am. Chem. Soc.* **134**, 4782–4789 (2012).
13. D. M. Lynn, R. Langer, Degradable poly(β-amino esters): Synthesis, characterization, and self-assembly with plasmid DNA. *J. Am. Chem. Soc.* **122**, 10761–10768 (2000).
14. J. J. Green, R. Langer, D. G. Anderson, A combinatorial polymer library approach yields insight into nonviral gene delivery. *Acc. Chem. Res.* **41**, 749–759 (2008).
15. D. G. Anderson, D. M. Lynn, R. Langer, Semi-automated synthesis and screening of a large library of degradable cationic polymers for gene delivery. *Angew. Chem. Int. Ed. Engl.* **42**, 3153–3158 (2003).
16. A. Akinc, D. G. Anderson, D. M. Lynn, R. Langer, Synthesis of poly(β-amino ester)s optimized for highly effective gene delivery. *Bioconjug. Chem.* **14**, 979–988 (2003).
17. J. J. Green, G. T. Zugates, N. C. Tedford, Y.-H. Huang, L. G. Griffith, D. A. Lauffenburger, J. A. Sawicki, R. Langer, D. G. Anderson, Combinatorial modification of degradable polymers enables transfection of human cells comparable to adenovirus. *Adv. Mater.* **19**, 2836–2842 (2007).
18. A. A. Eltoukhy, D. Chen, C. A. Alabi, R. Langer, D. G. Anderson, Degradable terpolymers with alkyl side chains demonstrate enhanced gene delivery potency and nanoparticle stability. *Adv. Mater.* **25**, 1487–1493 (2013).
19. M. Ahmed, R. Narain, The effect of molecular weight, compositions and lectin type on the properties of hyperbranched glycopolymers as non-viral gene delivery systems. *Biomaterials* **33**, 3990–4001 (2012).
20. C. C. Lee, J. A. MacKay, J. M. J. Fréchet, F. C. Szoka, Designing dendrimers for biological applications. *Nat. Biotechnol.* **23**, 1517–1526 (2005).
21. Y. Nakayama, Hyperbranched polymeric "star vectors" for effective DNA or siRNA delivery. *Acc. Chem. Res.* **45**, 994–1004 (2012).
22. M. Ahmed, B. F. L. Lai, J. N. Kizhakkedathu, R. Narain, Hyperbranched glycopolymers for blood biocompatibility. *Bioconjug. Chem.* **23**, 1050–1058 (2012).
23. R. Reul, J. Nguyen, T. Kissel, Amine-modified hyperbranched polyesters as non-toxic, biodegradable gene delivery systems. *Biomaterials* **30**, 5815–5824 (2009).
24. Z. Kadlecova, Y. Rajendra, M. Matasci, L. Baldi, D. L. Hacker, F. M. Wurm, H.-A. Klok, DNA delivery with hyperbranched polylysine: A comparative study with linear and dendritic polylysine. *J. Control. Release* **169**, 276–288 (2013).
25. H. Tian, W. Xiong, J. Wei, Y. Wang, X. Chen, X. Jing, Q. Zhu, Gene transfection of hyperbranched PEI grafted by hydrophobic amino acid segment PBLG. *Biomaterials* **28**, 2899–2907 (2007).
26. Z. Kadlecova, L. Baldi, D. Hacker, F. M. Wurm, H.-A. Klok, Comparative study on the in vitro cytotoxicity of linear, dendritic, and hyperbranched polylysine analogues. *Biomacromolecules* **13**, 3127–3137 (2012).
27. Y.-b. Lim, S.-M. Kim, Y. Lee, W.-k. Lee, T.-g. Yang, M.-j. Lee, H. Suh, J.-s. Park, Cationic hyperbranched poly(amino ester): A novel class of DNA condensing molecule with cationic surface, biodegradable three-dimensional structure, and tertiary amine groups in the interior. *J. Am. Chem. Soc.* **123**, 2460–2461 (2001).
28. Y. Liu, D. Wu, Y. Ma, G. Tang, S. Wang, C. He, T. Chung, S. Goh, Novel poly(amino ester)s obtained from Michael addition polymerizations of trifunctional amine monomers with diacrylates: Safe and efficient DNA carriers. *Chem. Commun.* **20**, 2630–2631 (2003).
29. M. L. Forrest, J. T. Koerber, D. W. Pack, A degradable polyethylenimine derivative with low toxicity for highly efficient gene delivery. *Bioconjug. Chem.* **14**, 934–940 (2003).
30. D. Wu, Y. Liu, X. Jiang, L. Chen, C. He, S. H. Goh, K. W. Leong, Evaluation of hyperbranched poly(amino ester)s of amine constitutions similar to polyethylenimine for DNA delivery. *Biomacromolecules* **6**, 3166–3173 (2005).
31. D. Wu,Y. Liu, X. Jiang, C. He, S. H. Goh, K. W. Leong, Hyperbranched poly(amino ester)s with different terminal amine groups for DNA delivery. *Biomacromolecules* **7**, 1879–1883 (2006).
32. Z. Zhong, Y. Song, J. F. J. Engbersen, M. C. Lok, W. E. Hennink, J. Feijen, A versatile family of degradable non-viral gene carriers based on hyperbranched poly(ester amine)s. *J. Control. Release* **109**, 317–329 (2005).
33. D. Wu, Y. Liu, L. Chen, C. He, T.-S. Chung, S. H. Goh, $2A_2$ + BB′B″ approach to hyperbranched poly(amino ester)s. *Macromolecules* **38**, 5519–5525 (2005).
34. D. Wang, T. Zhao, X. Zhu, D. Yan, W. Wang, Bioapplications of hyperbranched polymers. *Chem. Soc. Rev.* **44**, 4023–4071 (2015).
35. B. I. Voit, A. Lederer, Hyperbranched and highly branched polymer architectures—Synthetic strategies and major characterization aspects. *Chem. Rev.* **109**, 5924–5973 (2009).
36. C. J. Bishop, T.-M. Ketola, S. Y. Tzeng, J. C. Sunshine, A. Urtti, H. Lemmetyinen, E. Vuorimaa-Laukkanen, M. Yliperttula, J. J. Green, The effect and role of carbon atoms in poly(β-amino ester)s for DNA binding and gene delivery. *J. Am. Chem. Soc.* **135**, 6951–6957 (2013).
37. A. Akinc, D. M. Lynn, D. G. Anderson, R. Langer, Parallel synthesis and biophysical characterization of a degradable polymer library for gene delivery. *J. Am. Chem. Soc.* **125**, 5316–5323 (2003).
38. C. Chamorro, D. Almarza, B. Duarte, S. G. Llames, R. Murillas, M. García, J. C. Cigudosa, L. Espinosa-Hevia, M. J. Escámez, A. Mencía, A. Meana, R. García-Escudero, R. Moro, C. J. Conti, M. Del Río, F. Larcher, Keratinocyte cell lines derived from severe generalized recessive epidermolysis bullosa patients carrying a highly recurrent *COL7A1* homozygous mutation: Models to assess cell and gene therapies in vitro and in vivo. *Exp. Dermatol.* **22**, 601–603 (2013).
39. O. Veiseh, C. Sun, C. Fang, N. Bhattarai, J. Gunn, F. Kievit, K. Du, B. Pullar, D. Lee, R. G. Ellenbogen, J. Olson, M. Zhang, Specific targeting of brain tumors with an optical/magnetic resonance imaging nanoprobe across the blood–brain barrier. *Cancer Res.* **69**, 6200–6207 (2009).
40. H. S. Choi, Y. Ashitate, J. H. Lee, S. H. Kim, A. Matsui, N. Insin, M. G. Bawendi, M. Semmler-Behnke, J. V. Frangioni, A. Tsuda, Rapid translocation of nanoparticles from the lung airspaces to the body. *Nat. Biotechnol.* **28**, 1300–1303 (2010).
41. A. Schroeder, D. A. Heller, M. M. Winslow, J. E. Dahlman, G. W. Pratt, R. Langer, T. Jacks, D. G. Anderson, Treating metastatic cancer with nanotechnology. *Nat. Rev. Cancer* **12**, 39–50 (2012).
42. J. J. Green, J. Shi, E. Chiu, E. S. Leshchiner, R. Langer, D. G. Anderson, Biodegradable polymeric vectors for gene delivery to human endothelial cells. *Bioconjug. Chem.* **17**, 1162–1169 (2006).
43. X. M. Wang, X. Luo, Z. Y. Guo, Recombinant expression and downstream processing of the disulfide-rich tumor-targeting peptide chlorotoxin. *Exp. Ther. Med.* **6**, 1049–1053 (2013).
44. D. G. Anderson, W. Peng, A. Akinc, N. Hossain, A. Kohn, R. Padera, R. Langer, J. A. Sawicki, A polymer library approach to suicide gene therapy for cancer. *Proc. Natl. Acad. Sci. U.S.A.* **101**, 16028–16033 (2004).
45. B. Newland, A. Aied, A. V. Pinoncely, Y. Zheng, T. Zhao, H. Zhang, R. Niemeier, E. Dowd, A. Pandit, W. Wang, Untying a nanoscale knotted polymer structure to linear chains for efficient gene delivery in vitro and to the brain. *Nanoscale* **6**, 7526–7533 (2014).
46. J.-D. Fine, J. E. Mellerio, Extracutaneous manifestations and compilations of inherited epidermolysis bullosa: Part I. Epithelial associated tissues. *J. Am. Acad. Dermatol.* **61**, 367–384 (2009).
47. A. Fritsch, S. Loeckermann, J. S. Kern, A. Braun, M. R. Bösl, T. A. Bley, H. Schumann, D. von Elverfeldt, D. Paul, M. Erlacher, D. Berens von Rautenfeld, I. Hausser, R. Fässler, L. Bruckner-Tuderman, A hypomorphic mouse model of dystrophic epidermolysis bullosa reveals mechanisms of disease and response to fibroblast therapy. *J. Clin. Invest.* **118**, 1669–1679 (2008).
48. S. Heinonen, M. Mannikko, J. F. Klement, D. Whitaker-Menezes, G. F. Murphy, J. Uitto, Targeted inactivation of the type VII collagen gene (Col7a1) in mice results in severe blistering phenotype: A model for recessive dystrophic epidermolysis bullosa. *J. Cell Sci.* **112** (Pt. 21), 3641–3648 (1999).
49. Z. Siprashvili, N. T. Nguyen, M. Y. Bezchinsky, M. P. Marinkovich, A. T. Lane, P. A. Khavari, Long-term type VII collagen restoration to human epidermolysis bullosa skin tissue. *Hum. Gene Ther.* **21**, 1299–1310 (2010).
50. L. Cutlar, D. Zhou, Y. Gao, T. Zhao, U. Greiser, W. Wang, W. Wang, Highly branched poly(β-amino esters): Synthesis and application in gene delivery. *Biomacromolecules* **16**, 2609–2617 (2015).
51. J. Sunshine, J. J. Green, K. P. Mahon, F. Yang, A. A. Eltoukhy, D. N. Nguyen, R. Langer, D. G. Anderson, Small-molecule end-groups of linear polymer determine cell-type gene-delivery efficacy. *Adv. Mater.* **21**, 4947–4951 (2009).
52. A. Meana, J. Iglesias, M. Del Rio, F. Larcher, B. Madrigal, M. F. Fresno, C. Martin, F. San Roman, F. Tevar, Large surface of cultured human epithelium obtained on a dermal matrix based on live fibroblast-containing fibrin gels. *Burns* **24**, 621–630 (1998).
53. M. Del Rio, F. Larcher, F. Serrano, A. Meana, M. Muñoz, M. Garcia, E. Muñoz, C. Martin, A. Bernad, J. L. Jorcano, A preclinical model for the analysis of genetically modified human skin in vivo. *Hum. Gene Ther.* **13**, 959–968 (2002).
54. S. G. Lames, M. Del Rio, F. Larcher, E. García, M. García, M. J. Escamez, J. L. Jorcano, P. Holguín, A. Meana, Human plasma as a dermal scaffold for the generation of a completely autologous bioengineered skin. *Transplantation* **77**, 350–355 (2004).

Acknowledgments: We acknowledge A. South (Division of Cancer Research, University of Dundee, Ninewells, Dundee, UK) for providing the COL7A1 cDNA. We also acknowledge the technical support of A. Blanco of the Conway Flow Cytometry Core and D. Scholz of the Conway Electron Microscopy Core, University College Dublin. **Funding:** This work was funded by Science Foundation Ireland (SFI), a Technology Innovation and Development Award (14/TIDA/2367), an Industry Fellowship (15/IFA/3037), the Principal Investigator Program [10/IN.1/B2981(T)], an Investigator Award (12/IP/1688), the Health Research Board of Ireland (HRA-POR-2013-412), and the

National Natural Science Foundation of China (130-0401180007). The atomic force microscope used for this work was funded by SFI (SFI07/IN1/B931). **Author contributions:** Wenxin Wang, and D.Z. designed the experiments. D.Z., L.C., B. D., and Y.G. performed all the experiments. All authors were involved in the analyses and interpretation of the data. D.Z., L.C., J.O.-A., U.G., and Wenxin Wang, wrote the paper with the help of the co-authors. **Competing interests:** The authors declare that they have no competing interests. **Data materials and availability:** All data needed to evaluate the conclusions in the paper are present in the paper and/or the Supplementary Materials. Additional data will be made available by W.W. upon request.

Submitted 20 January 2016
Accepted 26 May 2016
Published 17 June 2016
10.1126/sciadv.1600102

Citation: D. Zhou, L. Cutlar, Y. Gao, W. Wang, J. O'Keeffe-Ahern, S. McMahon, B. Duarte, F. Larcher, B. J. Rodriguez, U. Greiser, W. Wang, The transition from linear to highly branched poly(β-amino ester)s: Branching matters for gene delivery. *Sci. Adv.* **2**, e1600102 (2016).

ScienceAdvances

The transition from linear to highly branched poly(#-amino ester)s: Branching matters for gene delivery

Dezhong Zhou, Lara Cutlar, Yongsheng Gao, Wei Wang, Jonathan O'Keeffe-Ahern, Sean McMahon, Blanca Duarte, Fernando Larcher, Brian J. Rodriguez, Udo Greiser, and Wenxin Wang

Sci. Adv. **2** (6), e1600102. DOI: 10.1126/sciadv.1600102